Effect of heat-treatment on corrosion performance of Ni and Ni-Cr-based alloys

Veronica Morudu[1*], *Nomsombuluko* Hadebe[1], *Marandela* Mulaudzi[1], and *Maje* Phasha[1]

[1]Mintek, Advanced Materials Division, 200 Malibongwe Drive, Randburg, 2125, South Africa

Abstract. Metal dusting is described as a severe form of corrosion attack in which iron, steels, nickel- and cobalt-based alloys disintegrate into metal or metal carbide particles in a coke deposit when exposed to strongly carburising gases (carbon activity ac>1) at elevated temperatures (300-800°C). Despite intense research efforts, which led to much progress in mitigating metal dusting, particularly in the oil and gas industry, the complete prevention still remains an issue. Current study focuses on measuring corrosion resistance of heat-treated austenitic Ni, Ni-Cr-based complex alloy compositions containing iron and copper as additional alloying elements.

1 Introduction

In its pure form, commercial nickel (Ni) finds application in caustic environments [1]. Due to its ability to dissolve significant amounts of various alloying elements to form solid solutions, a number of Ni alloy families have been developed so far depending on the intended specific application [1-3]. Ni alloys owe their exceptional corrosion resistance to a thin protective (passive) oxide film, which protects the underlying metal. Major alloying elements like chromium (Cr) and molybdenum (Mo) play a strong role in maintaining the passivity of the alloy and stabilising the passive film after a localised breakdown event. Consequently, the Ni alloys containing Cr and Mo are found to be suitable for use in a number of industrial applications, more specifically in environments where a high resistance to localised corrosion is of critical importance [4-5]. Chromium primarily forms a passive film of Cr_2O_3 on the surface, thereby imparting better passivation properties. Mo is known to inhibit localised corrosion by oxide formation within the pit, thereby retarding the pit growth. In the oil and gas industry, nickel-based alloys are the preferred choice in high-pressure and high-temperature environments containing large amounts of CO_2 and H_2S. Furthermore, Ni-based alloys are a good material choice for acid industries due to their high resistance to stress corrosion cracking (SCC), especially at high temperatures [6].

Improved corrosion-resistant alloys are widely in demand for different applications where the longevity and stability of the product is desired. However, when determining what alloy material to use for a given application, other factors such as cost and the underlying mechanical properties have to be taken into consideration. This matter gets complicated when the microstructure or composition is altered to attain suitable mechanical properties,

* Corresponding author: veronicam@mintek.co.za

subsequently affecting the corrosion resistance of the material. For example, tempering heat treatment is often applied to alloys in order to improve their toughness. However, this tempering process also makes the alloy more susceptible to corrosion by forming an increased amount of chromium carbides in the alloy [7].

Despite the high corrosion resistance of nickel-based alloys, corrosion types such as localised corrosion (particularly pitting or crevice corrosion), hydrogen embrittlement (HE) as well as metal dusting is still experience in the oil and gas industry due to extreme aggressiveness of the environment when sulphur and halide ions are present [4, 8-11]. It is this increasing demand by industry for alloys that possess corrosion resistance as well as high strength that leads to the need to develop new alloys [12].

Current commercially available best coating materials are Inconel alloys. However, it seems the high temperature heat resistance takes priority over corrosion resistance in the development of these alloys. This excellent heat resistance is attributed to high content of refractory elements (with brittle character), which also promotes formation of undesired sigma (σ) Ni_2Cr phase with a low coefficient of thermal expansion (CTE) compared to the austenitic matrix [13]. Consequently, resulting CTE mismatch has potential to become a crack-initiation point during shutdown cycles, thus causing material failure. This issue can be resolved by introducing inexpensive non-refractory elements such as copper (Cu) and iron (Fe) to austenitic Ni-Cr solid solution, to stabilize FCC phase at room temperature and improve corrosion resistance.

Thus in the current work, the alloys designed using density-functional-theory (DFT) based computational materials modelling software described elsewhere [13] were experimentally manufactured, heat-treated, characterized and tested under corrosion environment. Since the alloy 800 used as a substrate material for construction of reformers in petrochemical plants [14] has an austenitic structure, the suitable coating material needs also to be of face-centred cubic (FCC) crystal structure such as Ni-Cr-X (Cu, Fe) complex corrosion-resistant alloys that are mechanically stable at both low and high temperatures. This choice stems from the attempt to avoid formation of detrimental sigma (σ) and metal carbide phases. Precipitation of these brittle phases at elevated temperatures (300-800°C) depletes the alloying elements in the adjacent zones causing alloy sensitisation to intergranular corrosion [3, 8]. This focus of this study is to systematically track corrosion resistance performance against alloying and also investigate how this performance is affected by heat treatment.

2 Experimental procedure

The alloys were tailored for coating alloy 800 substrate, to enhance corrosion resistance properties. High purity elemental powder compositions were compacted and melted using the Button Arc Furnace (BAF) to produce alloys of different compositions. Figure 1 shows the image of the BAF used. BAF uses tungsten electrode to melt the sample on a continuous water-cooled copper hearth under argon atmosphere. Melted samples were turned 5 times to ensure chemical homogeneity. The samples were labelled as Ni, $Ni_{84}Cr_{16}$, HRA2 and HRC1. In both HRA2 and HRC1 alloys the Cr content was kept the same but HRA2 alloy contained Fe while HRC1 contained Cu, as shown in Table 1 below. Upon melting, the as-cast samples were sectioned to conduct analysis as well as for subjecting them under heat treatment process. The heat treatment process involved soaking the samples at 1200°C for 1 hour in the muffle furnace followed by either furnace cooling (FC) or water quenching (WQ). This temperature was chosen to achieve homogeneity as well as in attempt to avoid precipitation of Cr_2Ni and Ni_2Cr_3 chemical compounds [15]. The phase evolution were tracked using X-ray diffractometer (XRD).

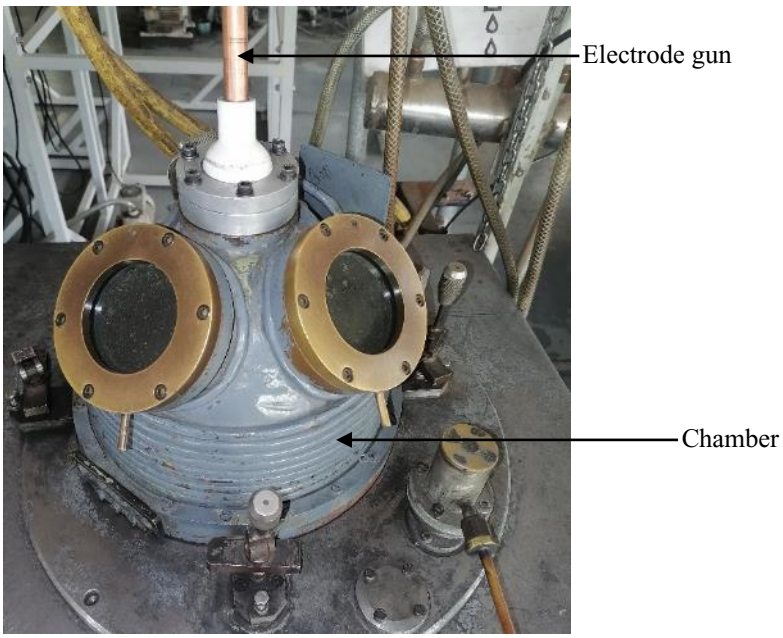

Fig. 1. Photographic image of the button arc melting furnace.

Table 1. List of alloys prepared and tested.

Alloys	Composition
Ni FC	Pure Nickel
Ni WQ	Pure Nickel
NiCr FC	$Ni_{84}Cr_{16}$
NiCr WQ	$Ni_{84}Cr_{16}$
HRA2 FC	NiCrMoWFe
HRA2 WQ	NiCrMoWFe
HRC1 FC	NiCuCrWMo
HRC1 WQ	NiCuCrWMo

2.1 Electrochemical corrosion testing

Electrochemical corrosion tests were carried out using potentiodynamic tests undertaken according to the ASTM Standard (ASTMG5, 2013). A PC-driven ACM Instruments AutoTafel potentiostat was used to perform the electrochemical tests. One graphite rod acted as counter-electrodes and a Haber-Luggin capillary made the junction with a saturated calomel reference electrode (SCE). All potential values were measured with respect to the SCE. The test was performed at 65±1°C in 5% NaCl + 0.5% acetic acid solution while stirring at 80rpm with a magnetic stirrer. Nitrogen was bubbled continuously during testing to remove all the oxygen and maintain an anaerobic condition. After each sample was immersed in the solution, the open circuit potential (OCP) against time curve was recorded for up to 1 hour. When the potential had reached a sufficiently stable value at 1 hours, a cyclic polarisation scan was recorded from –350 mV to 1500 mV at a scanning speed of 10 mV/min. The scan direction was not reversed. The corrosion rates were then calculated using Equation 1 below:

$$C_R = \frac{I_{Corr}.K.E_W}{D.A} \quad \text{----------} \quad [1]$$

where: C_R = The corrosion rates
Icorr = The corrosion current in amperes
K = A constant that defines the units for the corrosion rate
E_W = The equivalent weight in grams/equivalent
D = Density in grams/cm³
A = Area of the sample in cm²

3 Results and discussion

3.1 Phase evolution

XRD analysis was performed using a Malvern Panalytical Aeris diffractometer with PIXcel detector and fixed slits with Fe filtered Co-Kα radiation. The phases were identified using X'Pert Highscore plus software.
The phases present in the samples were detected through X-ray diffraction (XRD) analysis. The XRD patterns for Ni samples FC and WQ conditions are shown in **Error! Reference source not found.**. As expected, it evident that the crystal structure remains FCC in all conditions considered. Unsurprisingly, the FC sample has the highest peak intensity along both (111) and (200) planes of the FCC crystal, an indication of high crystallinity. Due of rapid cooling involved in the WQ sample, the peak intensities are much lower than in FC sample. The XRD patterns of the NiCr binary alloy are shown in **Error! Reference source not found.**. Similar to Ni samples FC and WQ the crystal structure remains FCC in all conditions and the FC sample has the highest peak intensity compared to the WQ. The XRD patterns of the HRA2 alloy are shown in **Error! Reference source not found.**. Despite the difference in peak heights, the XRD patterns of the FC and WQ samples are very similar as shown in **Error! Reference source not found.**(a) and (b). In addition, there is exist a common minute peak at approximately 53° 2θ position in both samples. According to peak matching, this peak is attributed to the presence of tetragonal phase with Cr_7Ni_3-type crystal structure space group #136. The lattice parameters of this phase are a= 0.871 nm and c = 0.449 nm, very close to those reported for Ni_2Cr_3 chemical compound (a= 0.882 nm and c = 0.458 nm) [15]. **Error! Reference source not found.** shows the XRD analysis of HRC1 alloy with the FC having the highest peak intensity due to grain growth compared to that of WQ sample. Besides the most dominant FCC phase in all these HRC1 samples, the presence of additional two phases is detected, namely, the tetragonal Cr_7Ni_3-type phase as well as the body centred cubic (BCC) phase. The BCC phase with distinct peaks at 48° and 70° 2θ positions, especially in the WQ sample, could be attributed to undissolved Mo or W probably as a result of the amount of Cu in the solid-solution.

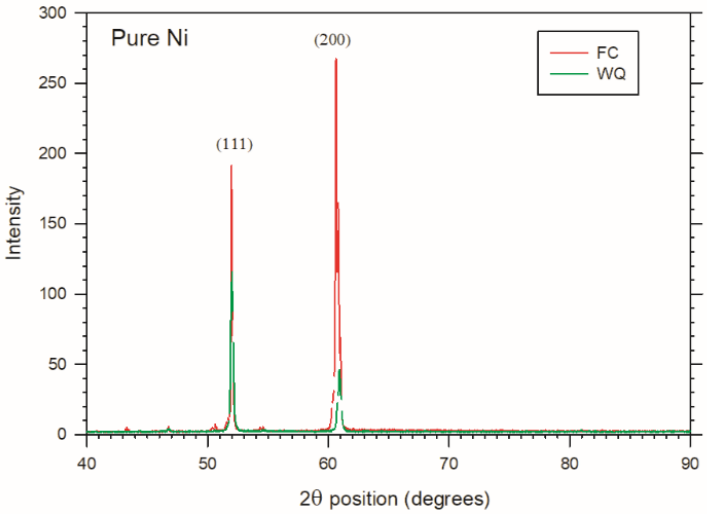

Fig. 2. X-ray spectrum of the pure Ni samples in the furnace cooled (FC) and water quenched (WQ) from soaking at 1200 °C.

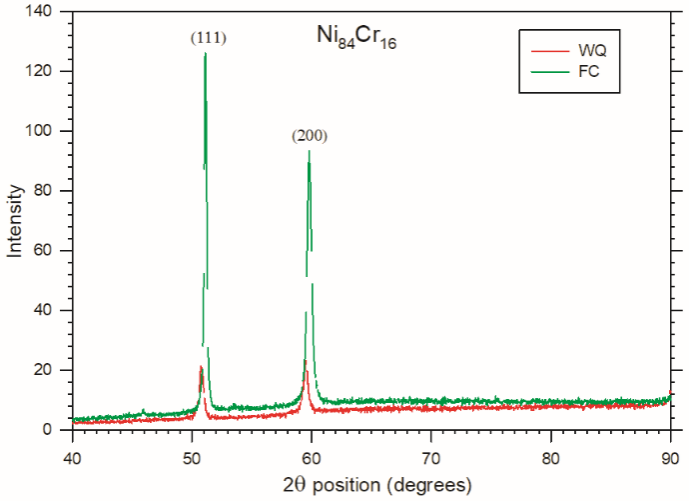

Fig. 3. X-ray spectrum of the NiCr samples in the furnace cooled (FC) and water quenched (WQ) from soaking at 1200 °C.

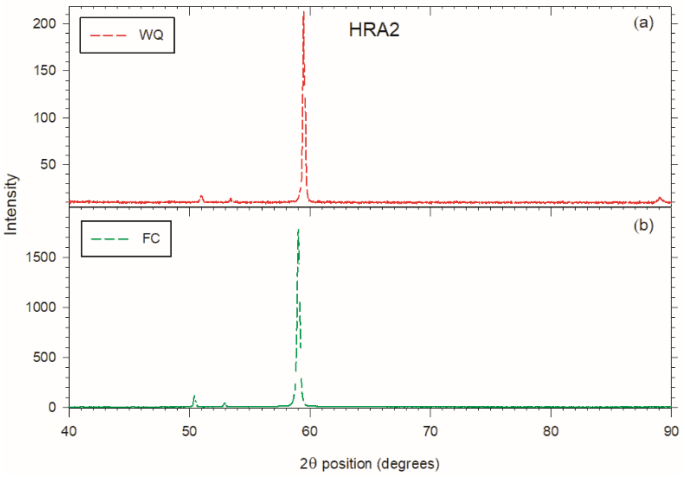

Fig. 4. X-ray spectrum of the HRA2 samples in the furnace cooled (FC) and water quenched (WQ) from soaking at 1200 °C.

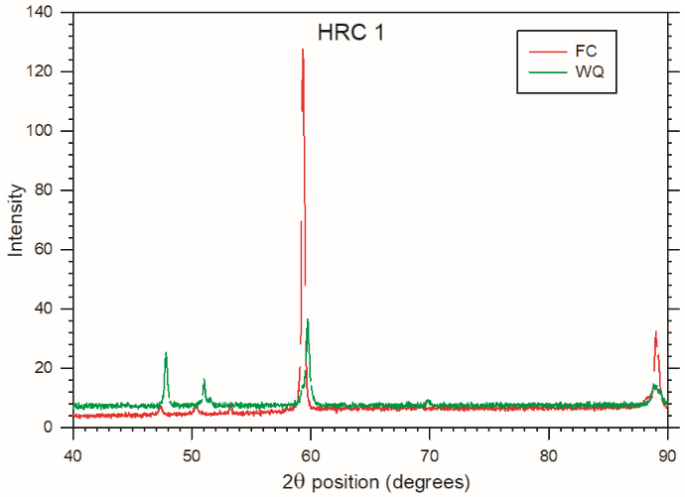

Fig. 5. X-ray spectrum of the HRC1 samples in as furnace cooled (FC) and water quenched (WQ) condition from soaking at 1200 °C.

3.2 Electrochemical corrosion

The potentiodynamic polarisation corrosion results of all the tested samples are shown in **Error! Reference source not found.** below and summarized in **Error! Reference source not found.**. It follows from these results that the corrosion rate in pure Ni was high compared to the other two alloys with complex concentrations. Ni sample subjected to WQ showed the highest corrosion rate in comparison to FC sample. Better corrosion resistance in the FC sample is likely to be associated with the presence of paramagnetic Ni particles which coexists along-side the abundant ferromagnetic Ni particles. When Ni was alloyed with Cr, Mo, W, together with Cu or Fe, the corrosion resistance increased significantly. For example, in the binary alloy containing 16 atomic percent (at.%) Cr, the corrosion resistance increases, more so upon WQ. Both FC and WQ HRA2 samples showed similar corrosion rates, an

indication that the heat treatment did not have an effect on the corrosion resistance of the alloy. On the other hand, the FC HRC1 sample showed higher corrosion rate compared to WQ HRC1 sample, which yielded the best corrosion resistance performance than all tested samples. In this sample, water quenching significantly improved the corrosion resistance. This behaviour is attributed to the amount of Cu that was kept within the matrix at high temperature, without affording it adequate time to segregate.

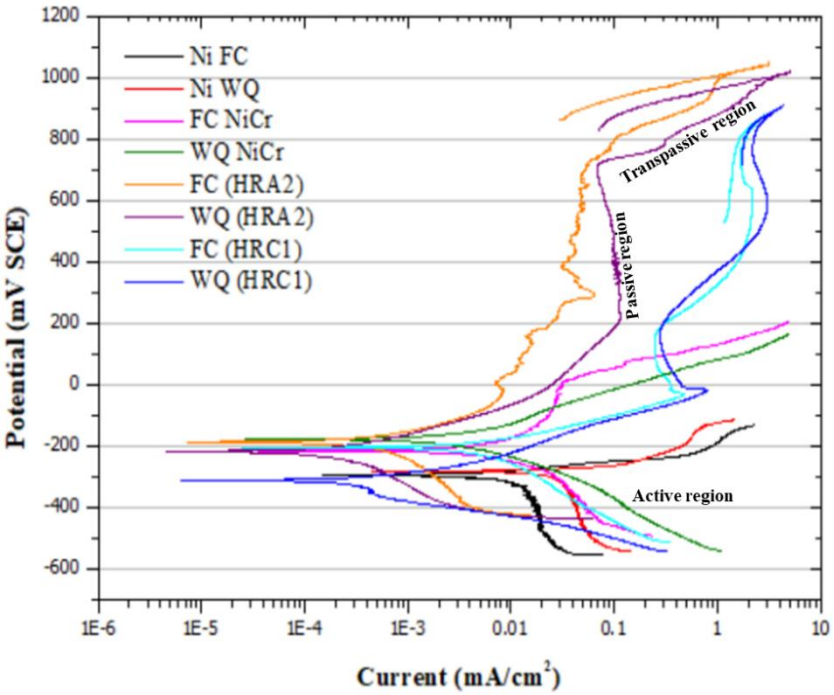

Fig. 6. Potentiodynamic polarisation curves of all the samples.

According to Fontana [16], the corrosion performance of both the FC and WQ Ni can be classified as good because the corrosion rates were 0.14 mm/ y and 0.42 mm/y respectively, which is in the range of 0.1 – 0.5 mm/y. As shown in **Error! Reference source not found.**, the FC and WQ HRA2 as well as WQ HRC1 have corrosion rates well below 0.02, therefore classified as having outstanding corrosion resistance performance. The FC HRC1 sample can be classified as exhibiting excellent corrosion resistance of 0.045mm/y which falls in the range of 0.02 – 0.1 mm/y according to Fontana criterion. The addition of alloying elements shifted the active region of pure Ni to the passive-transpassive region, as shown in **Error! Reference source not found.**.

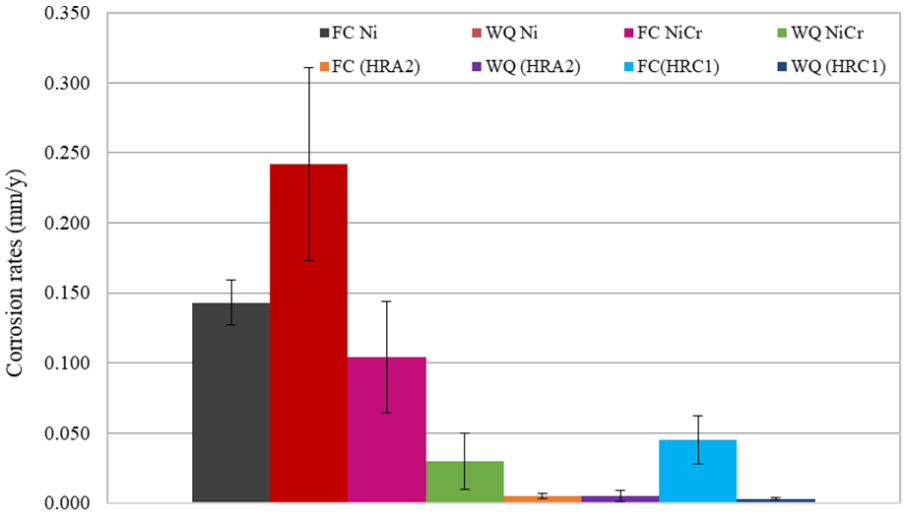

Fig. 7. Graphical representation of the corrosion rates.

4 Conclusion

In this work, it was possible to track the corrosion profile and effect of alloying on cast and heat-treated FCC Ni, Ni-Cr-based alloys bearing Fe and Cu. A better understanding of the effect of these alloying elements may aid in the optimised development of corrosion resistance alloys. This can be to the benefit of local petrochemical and oil & gas industry. When Ni was alloyed with Cr, Mo, W, together with Cu or Fe, the corrosion resistance increased significantly. Both FC and WQ HRA2 showed similar corrosion rates, an indication that the heat treatment did not have an effect on the corrosion resistance of the alloy. On the other hand, the FC HRC1 showed a slightly higher corrosion rate compared to WQ HRC1. The latter sample yielded the best corrosion resistance performance than all tested samples. The excellent corrosion resistance in the WQ HRC1sample is attributed to the amount of Cu that was kept in the matrix at high temperature, without affording it adequate time to segregate. Further work is underway to ascertain if the presence of tetragonal Cr_7Ni_3-type phase is responsible for this outstanding corrosion performance.

The authors would like to thank Mintek and the Advanced Metals Initiative (AMI) of the Department of Science and Innovation (DSI) for financial support. Ms Sibongile Masuku is acknowledged for her efforts in assisting with the electrochemical corrosion tests.

References

1. N.S. Zadorozne, C.M. Giordano, M.A. Rodríguez, R.M. Carranza and R.B. Rebak, Electrochim. Acta, **76**, 94 (2012)
2. P.E.A. Turchi, L. Kaufman and Z-K. Liu, Calphad: Comput. Coupling Ph. Diagr. Thermochem., **30**, 70 (2006)
3. R.M. Carranza and M.A. Rodríguez, npj Mater. Degred., **1,** 9 (2017)
4. A. Mishra, D. Richesin, and R.B. Rebak, Corr. Paper No. **5802**, Houston, TX: NACE International (2001)

5. E.C. Hornus, C.M. Giordano, M.A. Rodríguez, R.M. Carranza and R.B. Rebak, J. Electrochem. Soc., **162**, C105 (2015)
6. R. Karimihaghighi and M. Naghizadeh, Materials and Corrosion, **74**, 1246 (2023)
7. R Gonzalez, Electrochemical corrosion analysis of nickel-based superalloys, Master Thesis Report, Kth Ventenskap Konst, Stockholm, Sverige (2022)
8. J. Zhang, A. Schneider and G. Inden, Corr. Sci., **45**, 1329 (2003)
9. M.L. Holland and H.J. de Bruyn, International Journal of Pressure Vessel & Piping, **vol. 66**, 125 (1996)
10. H.J. de Bruyn and M.L. Holland, Corr. Paper No. **429**, NACE International, San Diego (1998)
11. M.L. Holland, Corr. Paper No. **01385**, NACE International, Houston, Texas (2001)
12. N.S. Zadorozne, M.A. Rodríguez, R.M. Carranza, N.S. Meck and R.B. Rebak, Paper No. 10236, Corrosion Conference & Expo, NACE International (2010)
13. M. Phasha, M. Mulaudzi and H. Möller, SA J. of Indust. Eng., **33**, 339 (2022)
14. M. Mulaudzi, L.A. Cornish, G.A. Slabbert and M.J. Papo, The Journal of The Southern African Institute of Mining and Metallurgy, **7A**, 589 (2012)
15. Y. Ustinovshikov, J. Alloys Compd., **543**, 227 (2012)
16. M.G. Fontana, Corrosion Engineering, Materials Science and Engineering Series, International Edition (1987)